Direct numerical simulation of supersonic boundary layer stabilization using grooved wavy surface

Ivan V. Egorov[1] and Andrey V. Novikov[2]
Central Aerohydrodynamic Institute (TsAGI), Zhukovsky, Moscow region, 140180, Russia

Alexander V. Fedorov[3]
Moscow Institute of Physics and Technology, Zhukovsky, Moscow region, 140180, Russia

Two-dimensional direct numerical simulation (DNS) of stabilization of supersonic boundary layers over a shallow grooved wavy plate at Mach=5.9 is carried out. Numerical experiments are conducted for propagation of disturbances generated by a suction-blowing actuator placed on the wall. Numerical data obtained for a flat plate are consistent with the linear stability theory (LST) and stability experiments in the "Transit-M" wind tunnel of the Institute of Theoretical and Applied Mechanics. It is shown that high-frequency forcing excites unstable disturbances in the flat-plate boundary layer relevant to the second-mode instability. The wavy wall leads to damping of these disturbances in a wide frequency band of the forcing.

Nomenclature

M	=	Mach number
Re	=	Reynolds number
γ	=	specific heat ratio
Pr	=	Prandtl number
x, y	=	longitudinal and vertical Cartesian coordinates
p	=	pressure
ρ	=	density
T	=	temperature
U	=	velocity magnitude
u, v	=	longitudinal and vertical Cartesian components of velocity vector
μ	=	dynamic viscosity
ω	=	forcing frequency
h	=	depth of the wall cavities

Superscripts

*	=	dimensional

Subscripts

∞	=	free stream
w	=	wall surface
n	=	normal to the wall

---

[1] Deputy Director, Aerothermodynamics department; e-mail: ivan_egorov@tsagi.ru
[2] Researcher, Aerothermodynamics department; e-mail: AndrewNovikov@yandex.ru
[3] Associate Professor, Department of Aeromechanics and Flight Engineering; e-mail: fedorov@falt.ru; Senior Member AIAA

I. Introduction

L AMINAR-turbulent transition leads to substantial increase of the aerodynamic drag and surface heating of supersonic vehicles. The ability to increase the laminar run is important for design and optimization of aerospace planes. Smoothing and shaping of the vehicle surface help to avoid early transition due to roughness, leading-edge contamination as well as cross-flow and Görtler instabilities. However, with these measures the laminar run may be still short because of the first and/or second mode instability. The wall cooling, which naturally occurs on hypersonic vehicle surfaces, strongly stabilizes the first mode while destabilizes the second mode. This indicates that hypersonic laminar flow control concepts should address the second-mode instability. In this connection, our study is focused on stabilization of the second mode. Since the most unstable second-mode waves are two-dimensional (2D), we perform 2D numerical simulation and do not address 3D disturbances.

Increasing of Mach number produces a stabilization effect on the flow in free shear layers and wakes. The amplification rates of shear-layer disturbances decrease significantly with the growth of compressibility as well known from numerous theoretical and experimental studies on stability of mixing layers and wakes (for example, Refs. 1, 2). These studies lead us to the assumption that a surface with local boundary-layer separations may stabilize the second mode. This hypothesis was motivated by computations[3,4] addressing stability of the flow over a rounded 5.5º corner. It was shown that the second-mode amplitudes decrease in a separated mixing layer. However there is effective excitation of acoustic disturbances in a relatively long separation bubble. They, in turn, generate the second-mode waves having appreciable initial amplitudes in the vicinity of reattachment point. We expect that with replacement of a long bubble by a sequence of small ones it is feasible to exploit the aforementioned stabilization effect and, at the same time, to avoid detrimental acoustic resonances within the bubbles.

In this paper we discuss results of direct numerical simulation (DNS) of unsteady two-dimensional hypersonic flow with local separations relevant to stability. The Navier–Stokes equations are solved numerically for disturbances generated by a local forcing (periodic suction-blowing) at the free-stream Mach number 5.9 in the near-wall flow with a sequence of small separation bubbles over a grooved plate.

II. Problem formulation and numerical method

The Navier–Stokes equations for 2D viscous compressible unsteady flows are solved numerically. The dimensionless conservative form of these equations is

$$\frac{\partial \mathbf{Q}}{\partial t} + \frac{\partial \mathbf{E}}{\partial \xi} + \frac{\partial \mathbf{G}}{\partial \eta} = 0 \,,$$

where (ξ, η) is a curvilinear coordinate system, $x = x(\xi, \eta)$, $y = y(\xi, \eta)$ are Cartesian coordinates, $\mathbf{Q}$ is a vector of conservative variables, $\mathbf{E}$ and $\mathbf{G}$ are flux vectors in the (ξ, η) coordinate system. These vectors are expressed in terms of the corresponding vectors $\mathbf{Q}_c$, $\mathbf{E}_c$, $\mathbf{G}_c$ in the Cartesian coordinate system as

$$\mathbf{Q} = J\mathbf{Q}_c \,, \quad \mathbf{E} = J\left(\mathbf{E}_c \frac{\partial \xi}{\partial x} + \mathbf{G}_c \frac{\partial \xi}{\partial y}\right), \quad \mathbf{G} = J\left(\mathbf{E}_c \frac{\partial \eta}{\partial x} + \mathbf{G}_c \frac{\partial \eta}{\partial y}\right)$$

where $J = \det\left[\partial(x,y) \,/\, \partial(\xi,\eta)\right]$ is the transformation Jacobian. Cartesian vector components for two-dimensional Navier–Stokes equations are

$$\mathbf{Q}_c = \begin{bmatrix} \rho \\ \rho u \\ \rho v \\ e \end{bmatrix}, \quad \mathbf{E}_c = \begin{bmatrix} \rho u \\ \rho u^2 + p - \tau_{xx} / \mathrm{Re}_\infty \\ \rho uv - \tau_{xy} / \mathrm{Re}_\infty \\ \rho uH - \dfrac{1}{\mathrm{Re}_\infty}\left(u\tau_{xx} + v\tau_{xy} + \dfrac{\mu}{\mathrm{Pr}(\gamma - 1)\mathrm{M}_\infty^2}\dfrac{\partial T}{\partial x}\right) \end{bmatrix}$$

$$
\mathbf{G}_c = \begin{bmatrix} \rho v \\ \rho uv - \tau_{xy}/\mathrm{Re}_\infty \\ \rho v^2 + p - \tau_{yy}/\mathrm{Re}_\infty \\ \rho vH - \dfrac{1}{\mathrm{Re}_\infty}\left(u\tau_{xy} + v\tau_{yy} + \dfrac{\mu}{\mathrm{Pr}(\gamma-1)\mathrm{M}_\infty^2}\dfrac{\partial T}{\partial y}\right) \end{bmatrix}.
$$

Here $e = p/(\gamma-1) + \rho(u^2 + v^2)/2$ is total energy; $H = T/\left((\gamma-1)\mathrm{M}_\infty^2\right) + \left[u^2 + v^2\right]/2$ is total specific enthalpy; τ is stress tensor with components

$$
\tau_{xx} = \mu\left(\frac{4}{3}\frac{\partial u}{\partial x} - \frac{2}{3}\frac{\partial v}{\partial y}\right), \ \tau_{xy} = \mu\left(\frac{\partial u}{\partial y} + \frac{\partial v}{\partial x}\right), \ \tau_{yy} = \mu\left(\frac{4}{3}\frac{\partial v}{\partial y} - \frac{2}{3}\frac{\partial u}{\partial x}\right).
$$

The fluid is a perfect gas with the specific heat ratio $\gamma = const$ and Prandtl number $\mathrm{Pr} = const$. The system of equations is closed by state equation $p = \rho T/(\gamma\,\mathrm{M}_\infty^2)$. The dynamic viscosity μ is calculated using Sutherland's formula $\mu = T^{3/2}(S+1)/(S+T)$, where $S = 110\,\mathrm{K}/T_\infty^*$. The second viscosity is assumed to be zero.

The dependent variables are normalized to the corresponding free-stream parameters: pressure – to the doubled dynamic pressure $\rho_\infty^* U_\infty^{*2}$; the coordinates – to the reference length L^* that is of the order of the plate length; time t – to L^*/U_∞^*. Computations were carried out at free-stream Mach number $\mathrm{M}_\infty = 5.9$, the Reynolds number $\mathrm{Re}_\infty = L^* U_\infty^* \rho_\infty^*/\mu_\infty^* = 1.435\times10^6$, $\gamma = 1.4$, $\mathrm{Pr} = 0.72$, $T_\infty^* = 43.08\,\mathrm{K}$, $T_w^* = 293\,\mathrm{K}$. These flow parameters correspond to the "Transit-M" wind tunnel of the Institute of Theoretical and Applied Mechanics (Novosibirsk) where stability experiments on similar configuration will be carried on in the nearest future. The dynamic viscosity μ is calculated using Sutherland's formula $\mu = T^{3/2}(S+1)/(S+T)$, where $S = 110\,\mathrm{K}/T_\infty^*$.

The Navier–Stokes equations are integrated numerically using an implicit finite-volume method with the second-order approximation in space and time. We use a quasi-monotonic Godunov-type scheme (TVD scheme) with Van-Leer limiter.[5] This gives a system of nonlinear algebraic equations, which is solved using the Newton iteration method. At every iteration step the corresponding linear system is solved using the GMRes method. Note that this approach is most efficient if the computational domain contains shock waves and other strong spatial inhomogeneities of the flow, such as boundary-layer separation. Despite dissipative nature of the TVD scheme, it was feasible to perform numerical simulations of boundary-layer receptivity[6] and stability[5] (including configurations with separation bubbles[4]), as well as the hypersonic laminar flow control using porous coatings.[7]

Computations are carried out for flow over a grooved wavy plate with 9 cavities. The surface shape is shown in Fig. 1 and given by the formula

$$
y(x) = \begin{cases} 0, & x < 0.4 \cup x > 1.2 \\ h\left|\cos\left(\pi(x-0.4)/0.1\right) - 1\right|, & 0.4 < x < 1.2 \end{cases}
$$

where the depth $h = 0.015$ approximately equals to the doubled boundary-layer thickness (2δ). For the considered flow parameters $\delta = 0.008$ at the station $x = 0.5$ located on the flat plate region.

The boundary conditions are: no-slip conditions on the lower boundary of computational domain ($u = v = 0$), the free-stream conditions on the left (inflow) and upper boundaries ($u = 1$, $v = 0$, $p = 1/\gamma\,\mathrm{M}_\infty^2$, $T = 1$), and a linear extrapolation from interior for the dependent variables u, v, p and T on the right (outflow) boundary ($f_i - 2f_{i-1} + f_{i-2} = 0$ – "soft" boundary conditions). The plate surface is isothermal with the temperature $T_w = 6.8$. Numerical simulations require an additional condition on the wall pressure. This condition is obtained by extrapolation of the near-wall pressure to the surface assuming that $\partial p_w/\partial n = 0$.

Computations are performed on a curved orthogonal grid with 2501×241 nodes. The grid is generated using numerical conformal mapping of a rectangle onto the computational domain.[8] It is clustered near the surface so that

3
American Institute of Aeronautics and Astronautics

55% of nodes are within the boundary layer or in the separation region with the mixing layer.

The problem is solved in two steps. First, a steady laminar flow field is computed using a time-dependent method. Then, unsteady disturbances are imposed onto the steady solution – a local periodic suction-blowing is introduced on the wall via the boundary condition for the mass-flow perturbation:

$$q_w\left(x,t\right) = \frac{\rho_w^* v_w^*}{\rho_\infty^* U_\infty^*} = \varepsilon \sin\left(2\pi \frac{x - x_1}{x_2 - x_1}\right)\sin\left(\omega t\right),\, x_1 \le x \le x_2,$$

where $x_1 = 0.05$ and $x_2 = 0.087$ are boundaries of the suction-blowing region.

The calculations were conducted at the different dimensionless forcing frequencies $\omega = \omega^* L^* / U_\infty^* = 100$, 125, 130, 135, 145, 150, 160, 165, 168, 175, 180 and 190. It was found that at $\omega = 168$ the actuator effectively generates the second-mode disturbance having its maximum amplitude near the outflow boundary of the computation domain. Other frequencies are investigated to clarify robustness of the stabilization using wavy walls. To ensure linear evolution of disturbances before separation and, hence, to perform comparisons with the linear stability theory (LST), we choose the forcing of small amplitude $\varepsilon = 10^{-3}$. Note that the numerical error of the steady solution should be much lower than the disturbance amplitude; i.e., the steady flow needs to be calculated with high accuracy.

In order to adapt the implicit scheme (suitable for steady problems) to simulations of unsteady flow fields, the following approach has been developed. At every time step the system of finite-difference equations is solved with prescribed accuracy that gives a quasi-steady solution at a particular time moment. With sufficiently small time intervals, a sequence of these solutions represents a solution of unsteady problem. The computation is continued until a time-periodic disturbance field sets in (this occurs at $t > 1.26$).

III. Numerical results

A. Steady flow

The computed steady-flow density field over a grooved wavy plate is shown in Figure 1. The viscous-inviscid interaction leads to formation of a shock wave in the leading-edge vicinity. Further downstream, the cavities induce oblique shocks whose interaction with the boundary layer gives recirculation zones inside the cavities (with negative horizontal velocity as shown in Fig. 2b). In the vicinity of each separation and reattachment points, a compression wave is clearly observed.

The upper boundary of each separation region is almost a straight line that is typical for supersonic flows. Thus the upper boundary of the whole mixing layer over the wavy plate remains almost unchanged compared to the flat plate case (Fig. 2a). Moreover the temperature in the vicinity of the grooved wavy surface is close to that in the flat-plate case (Fig. 3); i.e., cavities cause relatively small periodic temperature perturbations without average overheating. Therefore one may conclude that the chosen grooved surface weakly affects the global flow field over the boundary layer. At the same time this surface produces a mixing layer which bridges the cavities and resembles a free shear layer that is almost parallel. It is assumed that such a mixing layer could stabilize the boundary layer disturbances without detrimental effects.

B. Unsteady flow

At first disturbance evolution is computed for a flat plate. In this case, the computational domain is a rectangular of dimensions 1.25×0.27, the flow parameters and the boundary conditions are the same as in Section II. Several frequencies of the disturbance actuator were tested to choose the most suitable one. It was found that at $\omega = 168$ the second-mode instability is excited inside the computation domain and attains its maximum amplitudes near the outflow boundary. The suction-blowing actuator generates disturbances of a wide frequency band. The most powerful harmonics are slow and fast acoustic waves propagating downstream in the region between the plate surface and the bow shock. Inside the boundary layer these waves excite unstable disturbances.

A fragment of the instantaneous disturbance field (the difference between a disturbed flow field and a steady field) inside the boundary layer is shown in Fig. 4. For $x > 0.5$, the boundary-layer disturbance corresponds to the second mode, which is typified by two-cells in the pressure field and rope-like formations in the temperature field. The x-location of growth curve (the black line in Fig. 6) agrees with that predicted by the LST.[9] Furthermore the disturbance spectrum shown in Fig. 7 (the black line) is similar to that observed experimentally in "Transit-M" tunnel (private communication). Thus, the considered herein flow parameters are appropriate for analysis of the

American Institute of Aeronautics and Astronautics

second-mode disturbances. Furthermore, the numerical method can be used for direct simulations of the boundary-layer instability (this issue is discussed in Refs. 5, 4). Since the code provides numerical solutions of full Navier-Stokes equations, it can be also used for calculations of nonlinear disturbances in separation bubbles.

In the case of grooved plate, the disturbances over the mixing layer behave similar to the flat plate case (Fig. 5) because the upper boundary of mixing layer is weakly affected by the separation bubbles within the cavities. Inside the boundary layer, evolution of disturbances is completely different. As shown in Fig. 6 for the disturbance of fixed frequency $\omega = 168$, on a flat plate the second mode amplifies and reaches its maximum amplitude at $x \approx 0.93$, while on the grooved plate the disturbance damps sharply. Comparison of the disturbance spectra at the station $x = 0.9$ (Fig. 7) shows that the grooved surface produces stabilization effect in rather wide frequency band $140 < \omega < 190$.

Note that this positive effect was not observed in the previously investigated case of a relatively long separation bubble over the rounded compression corner.[4] It can be explained by comparison of the pressure disturbance fields inside the separation bubble. In the compression corner, a waveguide is formed inside a long separation zone and acoustic waves of appreciable amplitudes are excited via the resonance mechanism. These acoustic waves effectively generate the boundary-layer disturbances growing downstream from the reattachment point. For the configuration considered herein, the separation bubbles are relatively short that prevents from resonant excitation of acoustic disturbances within cavities (Fig. 8). Furthermore, the boundary-layer reattachments on the groove tops are smooth and relatively short that also prevents from the intensive second-mode growth in these regions.

IV. Conclusions

Stability of the separated supersonic near-wall flow over a grooved plate is simulated by means of numerical integration of two-dimensional Navier–Stokes equations. For this purpose, perturbations of the blow-suction type, local in space and harmonic in time, are introduced into the boundary layer upstream from the grooved region.

It is shown that high-frequency forcing effectively excites the second mode in the boundary layer flow. Upstream from the first separation bubble this unstable mode behaves like in the flat-plate case. Then it is stabilized over the grooved surface where the boundary-layer is transformed to the mixing layer bridging neighboring cavities.

The wavy surface weakly affects the acoustic component of disturbances in the boundary layer, i.e., the grooved plate does not produce detrimental effects associated with secondary reflections of acoustic waves in the separation regions. Such effects could lead to resonant amplification of disturbances and, as a consequence, trigger early transition. Nevertheless, this 2D simulation does not capture three-dimension structures such as Görtler vortices and streaks. This issue will be addressed by 3D DNS studies in the nearest future.

In summary, the numerical simulations confirm the concept of boundary-layer stabilization with the use of a wavy wall producing a relatively stable free shear layer at sufficiently high free-stream Mach numbers. This expectation will be validated by experiments to be conducted in the Transit-M tunnel.

References

[1]Lees, L., and Gold, H., "Stability of laminar boundary layers and wakes at hypersonic speeds. Part 1. Stability of laminar wakes," *Fundamental Phenomena in Hypersonic Flow*, No. 4, pp. 310-337, 1964.

[2]Lysenko, V. I., "Experimental studies of stability and transition in high-speed wakes," *J. Fluid Mech*, Vol. 392, pp. 1-26, 1999.

[3]Balakumar, P., Zhao, H., and Atkins, H., "Stability of Hypersonic Boundary-Layers over a Compression Corner," *AIAA Paper* No 2002 2848.

[4]Egorov, I. V., Fedorov, A. V., Novikov, A. V., "Numerical modeling of the disturbances of the separated flow in a rounded compression corner," *Fluid Dynamics*, Vol. 41, No. 4, pp. 521-530, 2006 (Translated from Izvestiya Rossiiskoi Academii Nauk, Mekhanika Zhidkosti i Gaza, No. 4, 2006, pp. 39–49).

[5]Egorov, I. V., Fedorov, A. V., and Soudakov, V. G., "Direct numerical simulation of disturbances generated by periodic suction-blowing in a hypersonic boundary layer," *Theoret. Comput. Fluid Dynamics*, Vol. 20, No. 1, pp. 41-54, 2006.

[6]Egorov, I. V., Fedorov, A. V., and Soudakov, V. G., "Direct numerical simulation of supersonic boundary-layer receptivity to acoustic disturbances," *AIAA Paper* No 2005-97.

[7]Egorov, I. V., Fedorov, A. V., Novikov, A. V., and Soudakov, V. G., "Direct numerical simulation of supersonic boundary-layer stabilization by porous coatings," *AIAA Paper* 2007-948, 2007.

[8]Driscoll, T. A., and Vavasis, S. A., "Numerical Conformal Mapping Using Cross-Ratios and Delaunay Triangulation," *SIAM J. Sci. Comput*, Vol. 19, No 6, pp. 1783 1803, 1998.

[9]Fedorov, A. V., and Khokhlov, A. P., "Prehistory of instability in a hypersonic boundary layer," *Theoret. Comput. Fluid Dynamics*, Vol. 14, No. 6, pp. 359-375, 2001.
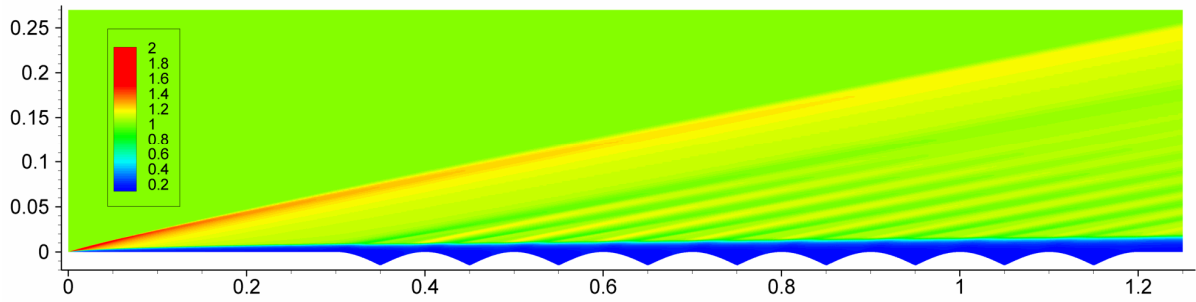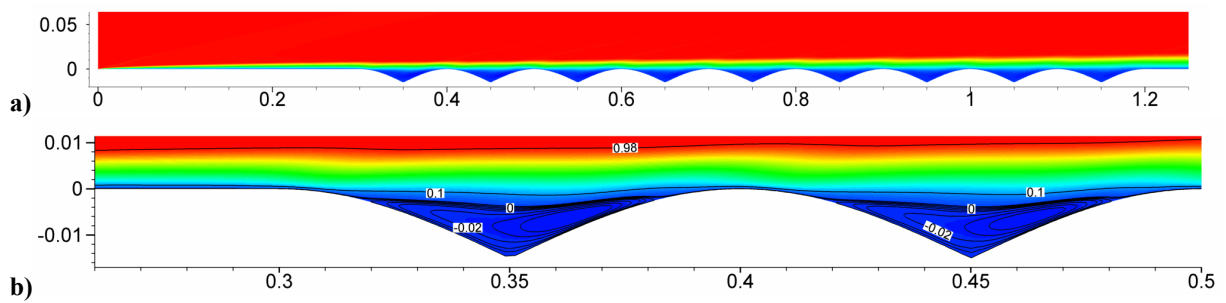
Figure 1. Density field of steady flow.

a)
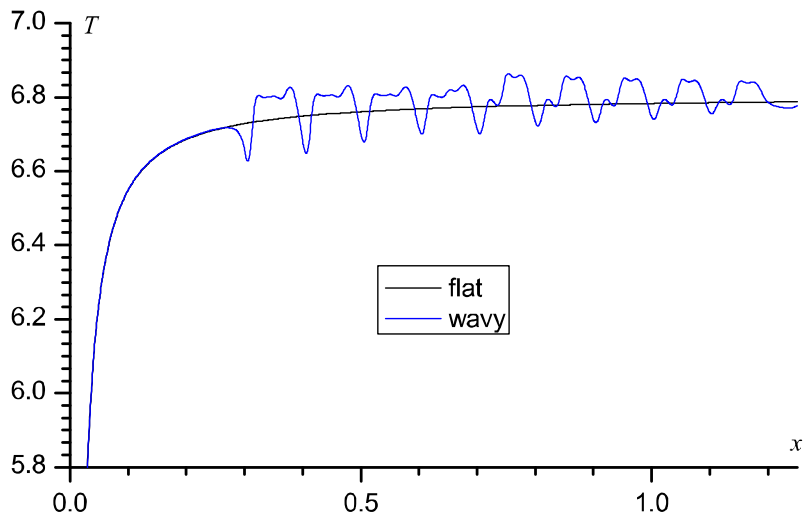
b)

Figure 2. Horizontal velocity field of steady flow.

Figure 3. Steady flow temperature distribution at the height 0.001 over the surface.

American Institute of Aeronautics and Astronautics
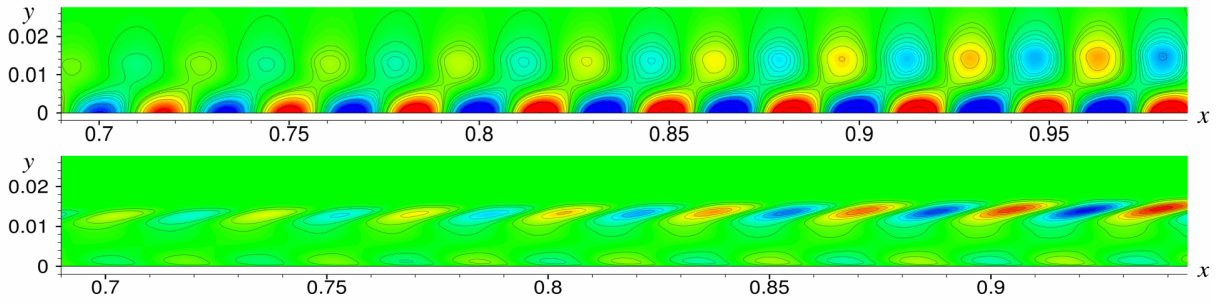
Figure 4. Fields of pressure (top) and temperature (bottom) disturbances over the flat plate for ω = 168 in the range of maximum growth rate.
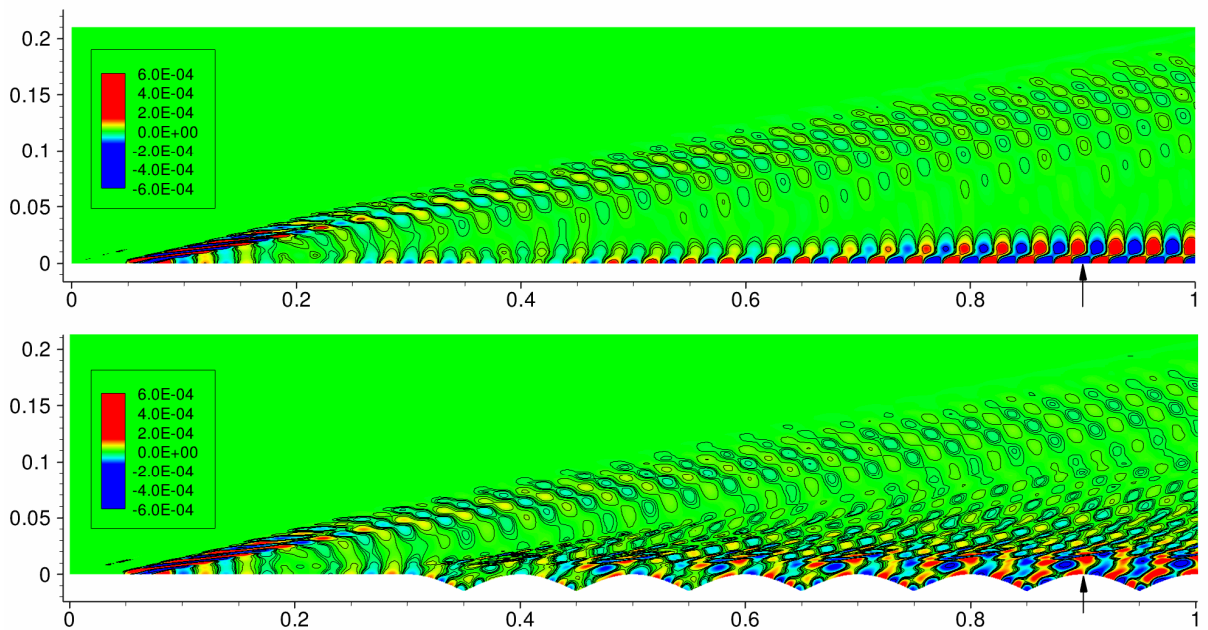

Figure 5. Pressure disturbance field over the flat (top) and wavy (bottom) plates for ω = 168. Arrow shows location of the sensor.
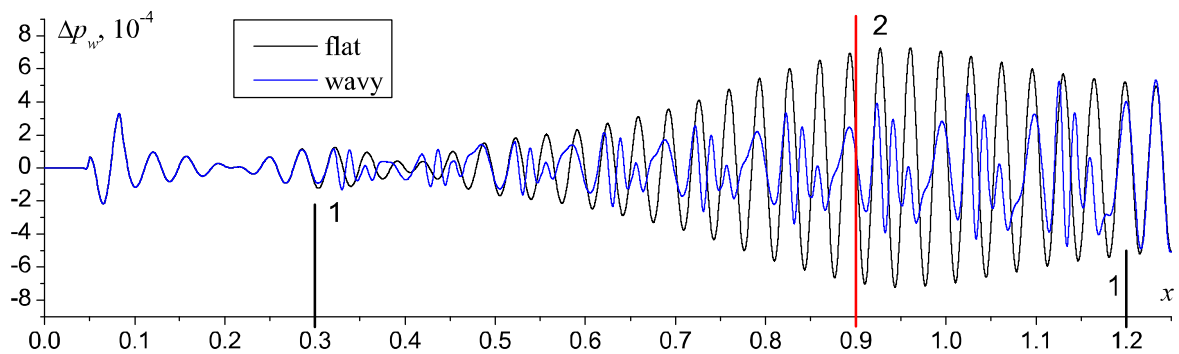

Figure 6. The wall pressure disturbance for ω = 168 at t = 1.5. 1 – boundaries of the grooved region, 2 – sensor location (x =0.9).
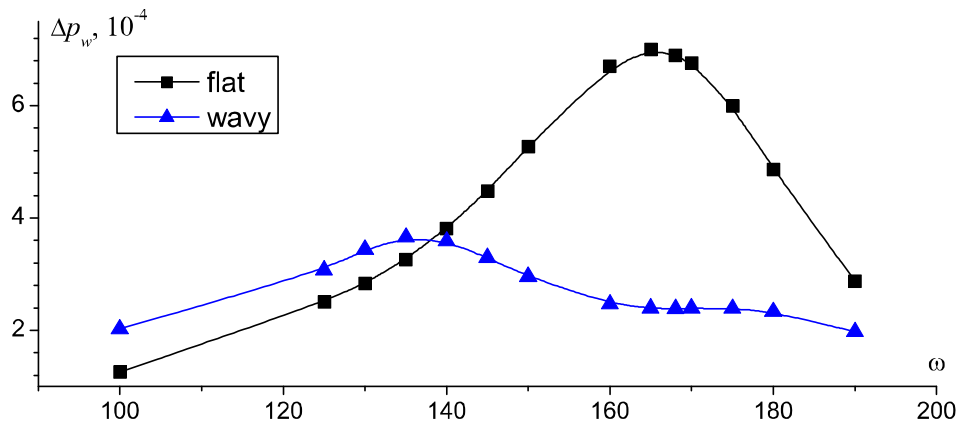
Figure 7. Spectrum of the wall pressure disturbance at the sensor station $x = 0.9$.
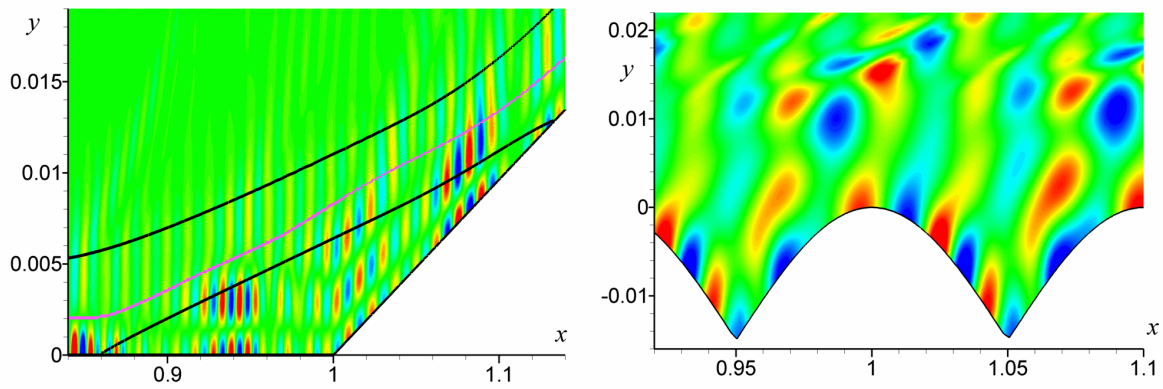

Figure 8. Pressure disturbance fields in separation bubbles over the compression corner[4] and inside cavities on the grooved plate.

American Institute of Aeronautics and Astronautics